

Volatility of linear and nonlinear time series

Tomer Kalisky,¹ Yosef Ashkenazy,² and Shlomo Havlin¹¹*Minerva Center and Department of Physics, Bar-Ilan University, Ramat-Gan, Israel*²*Solar Energy and Environmental Physics, BIDR, Ben-Gurion University, Midreshet Ben-Gurion, Israel*

(Received 14 June 2004; revised manuscript received 23 March 2005; published 21 July 2005)

Previous studies indicated that nonlinear properties of Gaussian distributed time series with long-range correlations, u_i , can be detected and quantified by studying the correlations in the magnitude series $|u_i|$, the “volatility.” However, the origin for this empirical observation still remains unclear and the exact relation between the correlations in u_i and the correlations in $|u_i|$ is still unknown. Here we develop analytical relations between the scaling exponent of linear series u_i and its magnitude series $|u_i|$. Moreover, we find that nonlinear time series exhibit stronger (or the same) correlations in the magnitude time series compared with linear time series with the same two-point correlations. Based on these results we propose a simple model that generates multifractal time series by explicitly inserting long range correlations in the magnitude series; the nonlinear multifractal time series is generated by multiplying a long-range correlated time series (that represents the magnitude series) with uncorrelated time series [that represents the sign series $\text{sgn}(u_i)$]. We apply our techniques on daily deep ocean temperature records from the equatorial Pacific, the region of the El-Ninō phenomenon, and find: (i) long-range correlations from several days to several years with $1/f$ power spectrum, (ii) significant nonlinear behavior as expressed by long-range correlations of the volatility series, and (iii) broad multifractal spectrum.

DOI: [10.1103/PhysRevE.72.011913](https://doi.org/10.1103/PhysRevE.72.011913)

PACS number(s): 87.10.+e, 89.20.-a, 89.65.Gh, 89.75.Da

I. INTRODUCTION

Natural systems often exhibit irregular and complex behavior that at first look erratic but in fact possesses scale invariant structure (e.g., [1,2]). In many cases this nontrivial structure points to long-range temporal correlations meaning that very far events are actually (statistically) correlated with each other. Long-range correlations are usually characterized by scaling laws where the scaling exponents quantify the strength of these correlations. However, it is clear that the two-point long-range correlations reveal just one aspect of the complexity of the system under consideration and that higher order statistics is needed to fully characterize the statistical properties of the system.

The two-point correlation function is in some cases used to quantify the scale invariant structure of time series (long-range correlations), while the q -point correlation function quantifies also the higher order correlations. In some cases the q -point correlation function is trivially related to the two-point correlation function—the scaling exponents of different moments are linearly dependent on the second moment scaling exponent. Processes with such correlation function are termed “linear” and “monofractal” since just a single exponent that determines the two-point correlations (and thus the linear correlations) quantifies the entire spectrum of q order scaling exponents. In other cases, the relation between the q -point correlation function has nontrivial relation to the two-point correlation function, and a (nontrivial) spectrum of scaling exponents is needed to quantify the statistical properties of the system; processes that have such nontrivial spectrum are called “nonlinear” and “multifractal.” The classification into linear and nonlinear processes is important for understanding the underlying dynamics of natural time series and for model development. Moreover, the nonlinear properties of natural time series may have practical diagnosis use (e.g., [3]).

Direct methods for measuring the multifractal spectrum [4–7] are rather complicated, involve advanced mathematical techniques (like the wavelet transform, see below), and require long time series. Recently, a simple measure for nonlinearity of time series was suggested [3]. Given a time series u_i , the correlations in the magnitude series (volatility) $|u_i|$ may be related (in some cases) to the nonlinear properties of the time series; basically, when the magnitude series is correlated the time series u_i is nonlinear. It was also shown that the scaling exponent of the magnitude series may be related, in some cases, to the multifractal spectrum width. However, these observations are empirical and the reasons underlying these observations still remain unclear.

Here we develop an analytical relation between the scaling exponent of the original time series u_i and the scaling exponent of the magnitude time series $|u_i|$ for linear series. We first show that when the original time series is nonlinear, the corresponding scaling exponent of the magnitude series is larger than (or in some cases equal to) the exponent of linear series and that the correlations in the magnitude series increase as the nonlinearity of the original series increases. These relations may help to identify nonlinear processes and to quantify their nonlinearity. Then, based on these results we suggest a generic model for multifractality by multiplying random signs with long-range correlated noise, and show that the multifractal spectrum width and the volatility exponent increase as these correlations become stronger. There are thus two objectives for the present study: (i) to provide a relation between the linearity/nonlinearity of the series under consideration and the long-range correlations in the magnitude series and (ii) to propose a generic model for multifractality.

The paper is organized as follows: in Sec. II we present some background regarding nonlinear processes and magnitude (volatility) series correlations. In Sec. III we develop an

analytical relation between the original time series scaling exponent α and the magnitude series exponent α_v ; we confirm the analytical relation using numerical simulation. We then study in Sec. IV the relation between volatility correlations and the multifractal spectrum width of several models with well known multifractal properties. Using both volatility and multifractal analysis we demonstrate the nonlinearity of deep ocean temperature time series from the equatorial Pacific. Finally, we introduce a simple model that generates multifractal time series by explicitly inserting long range correlations in the magnitude series. A summary of the results is given in Sec. V.

II. NONLINEARITY AND VOLATILITY CORRELATIONS

A. Two-point correlations

The long range correlations of a time series $\{u_i\}$ ($i = 0, 1, 2, \dots, N$) can be evaluated using the two-point correlation function $\langle u_i u_j \rangle$ ($\langle \cdot \rangle$ stands for expectation value); when u_i is long-range correlated and stationary the two-point correlation function is $\langle u_i u_j \rangle \sim |i-j|^{-\gamma}$ ($0 < \gamma < 1$) [8,9]. It is possible to estimate the scaling exponent of u_i using various methods, such as the power spectrum, fluctuation analysis (FA) [10], detrended fluctuation analysis (DFA) [2,10,11], wavelet transform [4], and others; see [8] for more details. These different techniques characterize the linear two point correlations in a time series with a scaling exponent which is related to the scaling exponent γ .

In this study we use the FA method for the analytical derivations since this method is relatively simple. In the FA method the sequence u_i is treated as steps of a random walk (i.e., $X_t = \sum_{i=0}^t u_i$); then the variance of its displacement is found by averaging over different time windows of length t . The scaling exponent α of the series (also referred to as the Hurst exponent H) can be measured using the relation $\text{var}(X_t) = \langle X_t^2 \rangle - \langle X_t \rangle^2 \sim t^{2\alpha}$ where $\text{var}(\cdot)$ is the variance; the scaling exponent α is related to the correlation exponent γ by $2 - \gamma = 2\alpha$.

B. High order correlations

A more complete description of the stochastic process $\{u_i\}$ with a zero mean is given by its multivariate distribution: $P(u_0, u_1, u_2, \dots)$. It is equivalent to the knowledge stored in the correlation functions of different orders [12,13]: $\langle u_i \rangle$, $\langle u_i u_j \rangle$, $\langle u_i u_j u_k \rangle$, $\langle u_i u_j u_k u_l \rangle$, etc. In many cases it is practical to use the cumulants of different orders C_q which are related to the q order correlation function by [13]:

$$C_1 = \langle u_i \rangle = 0, \quad (1)$$

$$C_2 = \langle u_i u_j \rangle, \quad (2)$$

$$C_3 = \langle u_i u_j u_k \rangle, \quad (3)$$

$$C_4 = \langle u_i u_j u_k u_l \rangle - \langle u_i u_j \rangle \langle u_k u_l \rangle - \langle u_i u_k \rangle \langle u_j u_l \rangle - \langle u_i u_l \rangle \langle u_j u_k \rangle, \quad (4)$$

and so on. Note that the first moment $\langle u_i \rangle$ in Eqs. (1)–(4) and throughout the paper is zero, to allow simpler analytical treatment.

For a linear process (sometimes referred to as “Gaussian” process), all cumulants above the second are equal to zero (Wick’s theorem) [13]. Thus, in this case, the two-point correlation fully describes the process [5,14], since all correlation functions (of positive and even order) may be expressed as products of the two-point correlation function $\langle u_i u_j \rangle$.

Processes that are nonlinear (or “multifractal”) have non-zero high order cumulants. The nonlinearity of these processes may be detected by measuring the multifractal spectrum [5,6] using advanced techniques, such as the wavelet transform modulus maxima [4] or the multifractal DFA (MF-DFA) [7]. In MF-DFA we calculate the q order correlation function of the profile $X_t = \sum_{i=0}^t u_i$ and the partition function is $Z_q(t) \equiv \langle |X_t|^q \rangle$. For time series that obey scaling laws the partition function is $Z_q(t) \sim t^{q\alpha(q)}$. Thus, the “spectrum” of scaling exponents $\alpha(q)$ characterizes the correlation functions of different orders. For a linear series, the exponents $\alpha(q)$ will all give a single value α for all q [7].

C. Volatility correlations

A known example for the use of volatility correlations (defined below) is econometric time series [15]. Econometric time series exhibit irregular behavior such that the changes (logarithmic increments) in the time series have a white noise spectrum (uncorrelated). Nonetheless, the *magnitudes* of the changes exhibit long-range correlations that reflect the fact that economic markets experience quiet periods with clusters of less pronounced price fluctuations (up and down), followed by more volatile periods with pronounced fluctuations (up and down). This type of correlation is referred to as “volatility correlations.”

Given a time series u_i , the magnitude (volatility) series may be defined as $|\Delta u_i| = |u_{i+1} - u_i|$. The scaling exponent of the magnitude series is the volatility scaling exponent α_v . Correlations in the magnitude series are observed to be closely related to nonlinearity and multifractality [3,16,17].

In this paper we refer to “volatility” with two small differences. First, we consider the *square* of the series elements rather than their absolute values. According to our observations, this transformation has negligible effect on the scaling exponent α_v , but it substantially simplifies the analytical treatment. Second, for simplicity, we also consider the series itself rather than the increment series. That is: the volatility series is defined as u_i^2 rather than $|\Delta u_i|$. Note that in most applications the absolute values of the increment series are considered instead of the absolute values of the series itself, since the original series is mostly nonstationary (defined below); here we overcome this problem by first considering stationary series. In the numerical and analytical analysis presented in this paper we use the time series u_i and the volatility series u_i^2 ; nevertheless, we introduce the series Δu_i ,

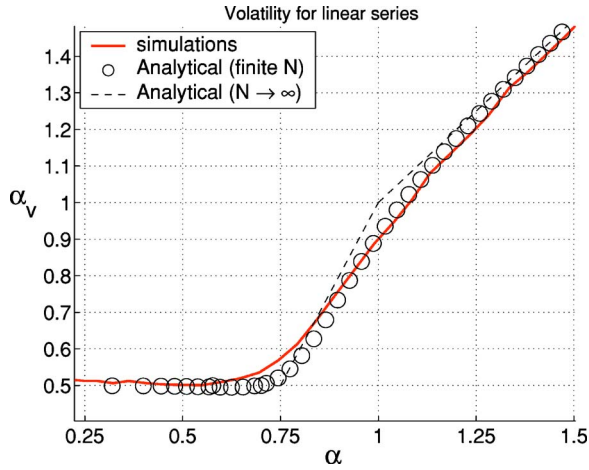


FIG. 1. (Color online) Magnitude series scaling exponent α_v vs the two-point correlation exponent α for linear sequences u_i . The solid line represents results for synthesized sequences of length 2^{15} , averaged over 15 configurations, for u_i^2 and $|u_i|$ (these two coincide). The circles represent the analytical reconstruction taking into account corrections due to finite size effects and nonstationarity. Analytical results for $N \rightarrow \infty$ are given by the dashed line.

$|\Delta u_i|$, and $|u_i|$ to enable comparison of the results presented here to those of previous publications.

D. Stationary and nonstationary time series

Series with correlation exponent $0 < \alpha < 1$ are *stationary*, meaning that their correlation function depends only on the *difference* between points i and j , i.e., $\langle u_i u_j \rangle = f(|i-j|)$, and their variance is a finite constant that does not increase with the sequence length. On the other hand, sequences with $\alpha > 1$ are *nonstationary* and have a different form of correlation function that depends also on the absolute indices i and j , $\langle u_i u_j \rangle = i^{2\alpha-2} + j^{2\alpha-2} - |i-j|^{2\alpha-2}$; see [8]. Scaling exponents of nonstationary series (or series with polynomial trends) may be calculated using methods that can eliminate constant or polynomial trends from the data [4,10,11].

III. VOLATILITY CORRELATIONS OF LINEAR TIME SERIES

We proceed to study the relation between the volatility correlation exponent α_v and the original scaling exponent α for linear processes, both numerically and analytically.

A. Simulations

We generate artificial long-range correlated linear sequences u_i with different values of α in the range $\alpha \in (0, 1.5]$ as follows [18]: (i) generate Gaussian white noise series, (ii) apply Fourier transform on that series, (iii) multiply the power spectrum $S(f)$ by $1/|f|^\beta$ where $\beta = 2\alpha - 1$ and $f \neq 0$, and (iv) apply inverse Fourier transform. The resultant series is long-range correlated with a scaling exponent α . We measure the volatility scaling exponent α_v , i.e., the scaling exponent of u_i^2 (and $|u_i|$), versus the original scaling exponent. The results are plotted in Fig. 1.

The simulations indicate that the dependence of α_v on α for linear series may be divided into three regions: for $\alpha < 3/4$ we obtain $\alpha_v \approx 1/2$, for $\alpha > 1.25$ we obtain $\alpha_v \approx \alpha$, while for $0.75 < \alpha < 1.25$ there is a transition region. These results were obtained using the DFA method which can handle nonstationary time series [19].

We note that for $\alpha > 1.25$ the series is highly nonstationary, i.e., it is most of the time either above or below 0, apart from few crossing points. Thus, the behavior of the series u_i is not very different from the behavior of its absolute value $|u_i|$, and therefore it is not surprising that $\alpha_v = \alpha$.

B. Analytical treatment

Let us consider a Gaussian distributed linear sequence u_i of length t with scaling exponent α . For simplicity, we assume that the sequence is stationary ($\alpha < 1$) and $\langle u_i \rangle = 0$. Consider the magnitude series: u_i^2 . In order to calculate the magnitude series scaling exponent α_v we will calculate the variance of the displacement $V_t = \sum_{i=0}^t u_i^2$:

$$\text{var}(V_t) = \langle V_t^2 \rangle - \langle V_t \rangle \langle V_t \rangle = \sum_{i=0}^t \sum_{j=0}^t [\langle u_i^2 u_j^2 \rangle - \langle u_i^2 \rangle \langle u_j^2 \rangle].$$

Because the series u_i is linear, the fourth cumulant is $C_4 = 0$ (Wick's theorem), and by using Eq. (4) we get,

$$\langle u_i^2 u_j^2 \rangle = \langle u_i^2 \rangle \langle u_j^2 \rangle + 2 \langle u_i u_j \rangle^2, \quad (5)$$

and thus,

$$\text{var}(V_t) = 2 \sum_{i=0}^t \sum_{j=0}^t \langle u_i u_j \rangle^2.$$

Substituting the two-point correlation function for long-range correlated time series:

$$\rho(i-j) = \langle u_i u_j \rangle \sim \begin{cases} |i-j|^{-\gamma} & i \neq j \\ 1 & i = j \end{cases} \quad (6)$$

we obtain

$$\text{var}(V_t) \sim t + \sum_{i \neq j} |i-j|^{-2\gamma} \sim t + t^{-2\gamma+2}. \quad (7)$$

Since $2 - \gamma = 2\alpha$ the above expression becomes

$$\text{var}(V_t) \sim t + t^{4\alpha-2} \equiv t^{2\alpha_v}. \quad (8)$$

For $\alpha < \frac{3}{4}$ the first term, t , is dominant and for $t \rightarrow \infty$ we obtain $\alpha_v = \frac{1}{2}$. Otherwise the second term, $t^{4\alpha-2}$, is dominating and thus $\alpha_v \approx 2\alpha - 1$. However, the simulation results (Fig. 1) deviate from $\alpha_v \approx 2\alpha - 1$ as $\alpha \rightarrow 1$. This is because as $\alpha \rightarrow 1$, logarithmic and polynomial corrections due to strong finite size effects and nonstationarity must be taken into account in our calculations (i.e., the variance of the sequence depends on its length; see the Appendix). This is done by dividing $\text{var}(V_t)$ [Eq. (8)] by the variance of the original sequence [20]:

$$\text{var}(u_i) = \frac{1}{1-\alpha} 2^{2\alpha-2} (1-t^{2\alpha-2}) \sim \begin{cases} \text{const} & \alpha \ll 1 \\ \ln t & \alpha = 1 \\ t^{2\alpha-2} & \alpha \gg 1. \end{cases} \quad (9)$$

This modification yields an α_v that is very close to the one obtained from the numerical simulation (in the transition region $0.75 < \alpha < 1.25$, and also for $\alpha > 1.25$ with $\alpha_v = \alpha$; see Fig. 1). The relation $\alpha_v = \alpha$ for $\alpha > 1.25$ can now be proved analytically: It is noticeable that the dominant scaling term of $\text{var}(V_t^2)$ for the nonstationary case is proportional to $t^{4\alpha-2}$ [Eq. (8)]. Dividing by the variance term, $t^{2\alpha-2}$ [Eq. (9)], yields $t^{2\alpha} \sim t^{2\alpha_v}$ and hence $\alpha = \alpha_v$.

IV. VOLATILITY CORRELATIONS AND THE MULTIFRACTAL SPECTRUM WIDTH

A. Random multifractal cascades

Following [3,17], we study the relation between the volatility scaling exponent α_v and the multifractal spectrum width of nonlinear multifractal time series. We generate artificial noise with multifractal properties according to the algorithm proposed in [16]; the multifractal properties of these synthetic time series are known analytically and thus enable us to study in detail the nonlinear measure of volatility correlations (see also [17]). The algorithm is based on random cascades on wavelet dyadic trees. The multifractal series is constructed by building its wavelet coefficients at different scales recursively, where at each stage the coefficients of the coarser scale are multiplied by a random variable W in order to build the coefficients of the finer scale. Note that we now consider the increments series of these artificial series, hence the generated time series is stationary. The multifractal spectrum $f(\alpha)$ depends on the statistical properties of the random variable W .

We choose W to follow the log-normal distribution, such that $\ln|W|$ is normally distributed, with μ and σ^2 being the mean and variance, respectively. For this case the multifractal spectrum $f(\alpha)$ is known analytically [16] and by assigning $f(\alpha)=0$ it is possible to obtain $\alpha_{\min, \max}$,

$$\alpha_{\min} = -\frac{\sqrt{2}\sigma}{\sqrt{\ln 2}} - \frac{\mu}{\ln 2}, \quad (10)$$

$$\alpha_{\max} = \frac{\sqrt{2}\sigma}{\sqrt{\ln 2}} - \frac{\mu}{\ln 2}. \quad (11)$$

Thus, the multifractal width, $\Delta\alpha = \alpha_{\max} - \alpha_{\min} = 2(\sqrt{2}\sigma/\sqrt{\ln 2})$, depends just on σ while the scaling exponent $\alpha(0)$ depends on μ , i.e., $\alpha(0) = -(\mu/\ln 2)$ [16].

Using the above algorithm, we generate multifractal time series with a fixed multifractal width $\Delta\alpha$ (by fixing σ) and different scaling exponents $\alpha(q=2)$ (by changing μ), and calculate their volatility exponents α_v (see Fig. 2) [21]. We find that the volatility correlation exponent is almost constant for $\alpha < 3/4$ indicating that the nonlinear properties of the series u_i do not change, which is consistent with the fact that the multifractal spectrum width remains the same (constant σ). We perform the same analysis for the respective surro-

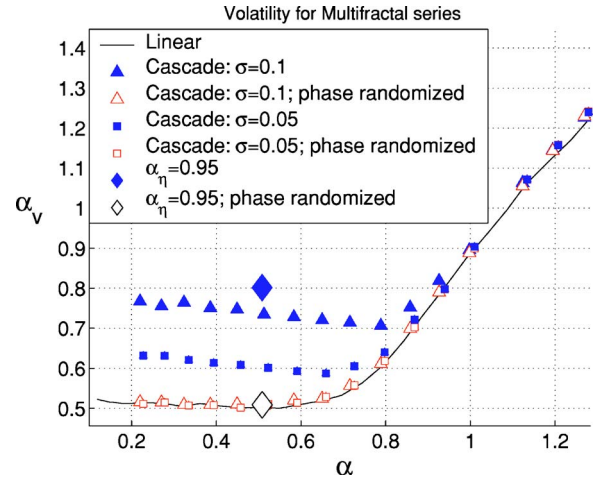


FIG. 2. (Color online) The magnitude series exponent α_v vs the two-point correlation exponent α for multifractal series. The full triangles and squares represent sequences generated by the log-normal random cascade algorithm with $\sigma=0.1$ (triangles) and $\sigma=0.05$ (squares); the multifractal spectrum of these examples is known analytically indicating that as σ increases the nonlinearity strengthens. The respective linear (phase randomized) surrogate data sequences are represented by empty symbols. The solid line indicates simulation results for linear sequences as derived in [17], explained in Sec. III, and shown in Fig. 1. The full diamond represents the scaling exponent of our multifractal model's sequences $u_i = \epsilon_i \eta_i$ with $\alpha_\eta = 0.95$, while the empty diamond represents the respective scaling exponent of the surrogate data. All sequences are of length 2^{14} elements, and results were averaged over 15 configurations. Error bars are smaller than symbol size.

gate time series, which are linearized series (after phase randomization) that have the same two-point correlations with exponent $\alpha(q=2)$ as the original series [22]. We find that the volatility exponent α_v , calculated in Sec. III for the linear case, is the lower bound for all multifractal sequences (studied here) with same $\alpha(q=2)$. Nonetheless, for $\alpha(q=2) > 1$, i.e., for nonstationary series, $\alpha_v = \alpha(q=2)$ as in linear series. It is clearly seen in Fig. 2 that for stationary time series [$\alpha(2) < 1$], the volatility correlations increase as the multifractal spectrum width becomes wider (larger σ value), or alternatively, as the nonlinearity of the original series strengthens.

B. Natural data example: Deep ocean temperature time series

As a simple example for the applicability of volatility analysis, we analyze deep water (500 m) temperature records taken from moored ocean buoys in the equatorial Pacific [23], see example in Fig. 3. The equatorial Pacific is the region of El-Niño, a known nonlinear phenomenon that has an important impact on the climate system. We consider the deep ocean temperature since it hardly shows seasonal periodicity, so that the scaling techniques we use will not need any preprocessing.

Using the DFA method to measure the correlation exponent of our series, we find that the temperature series T_i is strongly correlated: $\alpha \approx 1$, see Fig. 4. The volatility series

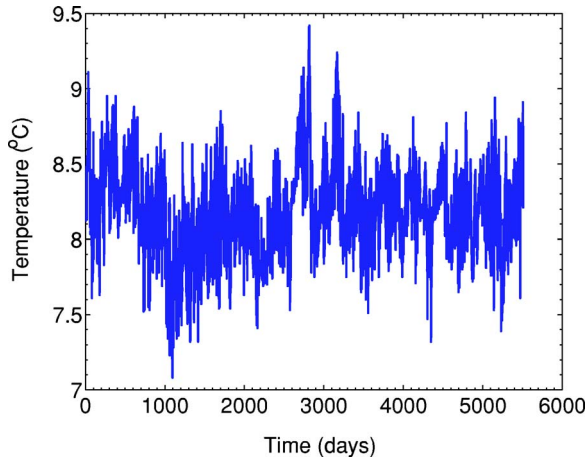


FIG. 3. (Color online) Deep water (500 m) temperature time records from the equatorial Pacific, as measured by a moored ocean buoy located on the equator at 170°W , during the years 1990–2004. Data record consists of 5513 points, each point representing one day.

exponent (i.e., the scaling exponent of the absolute value of the increments $|\Delta T_i|$) is $\alpha_v \approx 0.72$ indicating that our series is indeed multifractal, which is consistent with multifractal analysis using MF-DFA [7] shown in Fig. 5. We obtain similar results for the several data sets available from the equatorial Pacific (5 time series from 500 m depth).

C. A simple model for multifractality

We now propose a simple model for generating multifractal records, based on the property that multifractal series exhibit long range correlations in the volatility series. Following [24], we multiply a long range correlated series η_i (with a scaling exponent $\alpha_\eta > 0.75$) with a series of uncorrelated

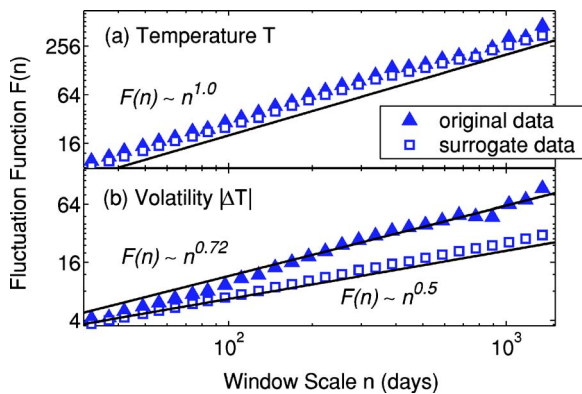


FIG. 4. (Color online) Volatility analysis of deep ocean temperature records. (a) The fluctuation function $F(n) = \text{var}(X_n) \sim n^\alpha$ of the profile as a function of the window n . Window size is measured in days. Both the original and surrogate (i.e., phase-randomized) series are strongly correlated and exhibit the same scaling exponent $\alpha \approx 1$. (b) The magnitude series of the increments of the original data are correlated ($\alpha > 1/2$) indicating that it is nonlinear, whereas the magnitude series of the surrogate data [22] are uncorrelated ($\alpha = 1/2$) hence indicating that it is linear.

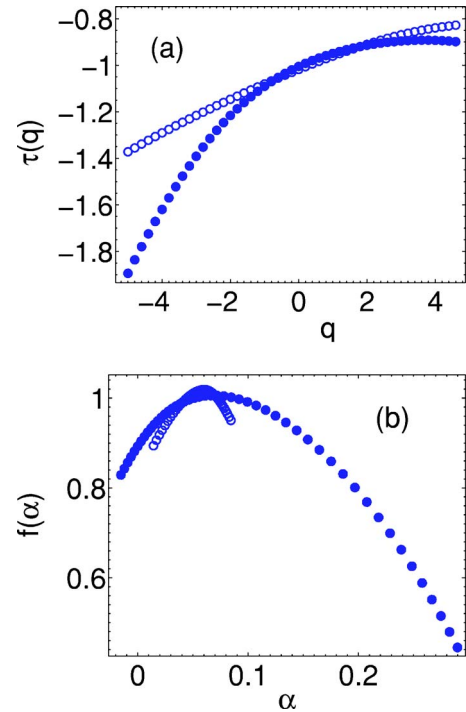


FIG. 5. (Color online) Multifractal analysis of deep ocean temperature records using the MF-DFA method [7]. (a) The exponents $\tau(q)$ give the scaling of the different moments: $Z_q(n) \equiv \langle |X_n|^q \rangle \sim n^{\tau(q)}$, where n is the window size. In these measurements the exponents $\tau(q)$ were calculated for window scales between 8 days and 512 days, with DFA order 3 (see [7] for details). The curvature in $\tau(q)$ for the original series (\bullet) reflects the multifractality of the series. On the other hand, for the surrogate series (\circ) $\tau(q)$ is much closer to linear [i.e., $\tau(q) = q\alpha$] indicating that it is monofractal and that a single exponent α characterizes all moments. (b) The multifractal spectrum $f(\alpha)$ is much broader for the original data (\bullet) compared to the surrogate data (\circ).

random signs $\epsilon_i = \pm 1$. The resultant series, $u_i = \epsilon_i \eta_i$, has a two-point correlation exponent $\alpha = 1/2$ because of the random signs ϵ_i . The magnitude exponent α_v is the same as the magnitude exponent $\alpha_{v,\eta}$ for η_i , because $|u_i| = |\eta_i|$. Thus, using our results from Sec. III, if we take $\alpha_\eta > 0.75$ we get a sequence with $\alpha = 1/2$ and $\alpha_v \approx 2\alpha_\eta - 1 > 1/2$ (see Fig. 2, full diamond symbol for $\alpha_\eta = 0.95$). Note that in Fig. 2 the theoretical value of $\alpha_v = 2 \times 0.95 - 1 = 0.9$ is higher than that of the numerical estimation $\alpha_v = 0.8$, most probably due to finite size effects.

According to our derivation in Sec. III, this sequence is nonlinear/multifractal (because linear series with a two-point correlation exponent $\alpha = 1/2$ should have $\alpha_v = 1/2$). Indeed, one can see from Fig. 6 that the multifractal width for this model increases as α_η increases beyond 0.75.

Natural processes are often characterized by complex nonlinear and multifractal properties. However, the underlying mechanisms of these processes are usually not so well understood. Several prototypes for multifractal processes include, e.g., (i) the energy cascade model describing turbulence [4,14], (ii) the *universal multifractal process* usually used to generally explain geophysical phenomena [25,26], and (iii) the turbulence-like model for heart rate variability [27].

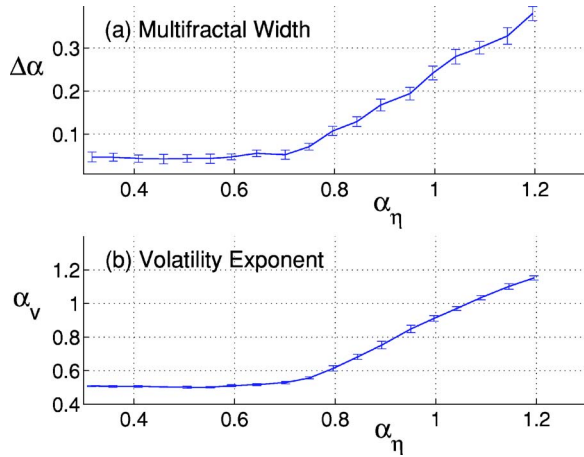


FIG. 6. (Color online) (a) Multifractal spectrum width and (b) volatility exponent α_v for sequences of the form $u_i = \epsilon_i \eta_i$ of length 2^{19} , averaged over 15 configurations. The error bars indicate the mean ± 1 std. For $\alpha_\eta > 0.75$ both the volatility correlation exponent and the multifractal spectrum width of the series are increasing with α_η .

The multifractal model described in this section is a simple model with known properties that may help to gain better understanding of multifractal processes. The model consists of two components as follows: (i) a random series (which can be also any other long-range correlated series) that may represent fast processes of a natural system, which as a first approximation may be regarded as a white noise, interacting with (ii) a long-range correlated process that may represent a slow modulation of the natural system. This interaction results in episodes with less volatile fluctuations followed by episodes with more volatile fluctuations. In the context of heart-rate variability, the fast component may represent the parasympathetic branch of the autonomic nervous system while the slow process may represent the sympathetic and the hormonal activities. In the context of geophysical phenomena, the fast component may represent the fast atmospheric processes [28] while the slow process may represent the relatively slow oceanic processes. Our model can also be used to describe other complex systems like economy and network dynamics.

V. SUMMARY

We study the behavior of the magnitude series scaling exponent α_v versus the original two-point scaling exponent α for linear and nonlinear (multifractal) series. We find analytically and by simulations that for linear series the dependence of α_v versus α may be divided into three regions: for $\alpha < 3/4$ the volatility exponent is $\alpha_v = 1/2$, for $\alpha > 1.25$ the volatility exponent is $\alpha_v = \alpha$, while for $0.75 < \alpha < 1.25$ there is a transition region in which logarithmic corrections due to finite size effects and nonstationarity are dominant.

The results presented here provide the theory for the relation found previously [3,17] between multifractality and the scaling exponent of the magnitude of the differences series (volatility). This relation provides a simple method for

preliminary detection and quantification of nonlinear time series, a procedure which usually requires relatively complex techniques and long experimental records. We also demonstrate the use of volatility analysis on deep ocean temperature records (500 m depth in the equatorial Pacific), and show that they exhibit significant nonlinearity.

We also study the volatility of some known models of multifractal time series (with analytically known multifractal properties), and find that their magnitude scaling exponent is bounded from below by α_v of the corresponding phase randomized linear surrogate series; i.e., the volatility scaling exponent α_v is larger than (or equal to) the scaling exponent of linear series with the same two-point correlations.

Based on the above findings, we propose a simple model that generates multifractal series by explicitly inserting long range correlations ($\alpha_\eta > 0.75$) into the magnitude series. This model may serve as a generic model for multifractality and may help to gain preliminary understanding of natural complex phenomena. The model, which involves interaction between fast and slow components, may represent natural fast processes that interact with slower processes. In addition, the simplicity of the model may help to identify these processes more easily in experimental records.

ACKNOWLEDGMENTS

We wish to thank Yshai Avishai for useful discussions and the Israeli Center for Complexity Science for financial support.

APPENDIX: FINITE SIZE EFFECTS AND NONSTATIONARITY NEAR $\alpha=1$

A linear time sequence with scaling exponent α can be generated by filtering Gaussian white noise such that the power spectrum will be [18]:

$$S(f) \sim \begin{cases} 0 & f = 0 \\ \frac{1}{|f|^\beta} & f \neq 0 \end{cases} \quad (\text{A1})$$

where $\beta = 2\alpha - 1$. Assume a signal u_i of N discrete points sampled at time intervals Δt . The power spectrum consists of N points in the frequency range $(-1/2\Delta t, 1/2\Delta t]$ with intervals of $\Delta f = 1/N\Delta t$. Thus, looking only at the positive frequencies, the minimal frequency (without loss of generality) is $\Delta f/2 = 1/2N\Delta t$. The variance of the signal is the total area under the power spectrum:

$$\text{var}(u_i) = 2 \int_{1/2N\Delta t}^{1/2\Delta t} S(f) df = 2 \int_{1/2N\Delta t}^{1/2\Delta t} \frac{1}{f^{2\alpha-1}} df. \quad (\text{A2})$$

Assuming $\Delta t = 1$, for $\alpha = 1$ the variance is,

$$\text{var}(u_i) = 2 \ln N. \quad (\text{A3})$$

Thus, the variance diverges logarithmically for $\alpha = 1$.

For $\alpha \neq 1$ the variance is

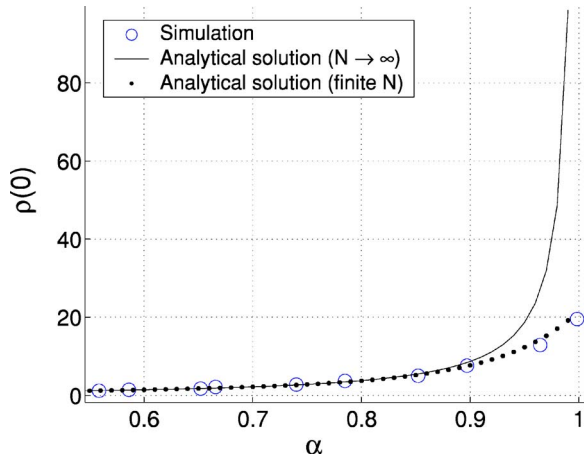


FIG. 7. (Color online) Correlation coefficient $\rho(0)$ [i.e., the variance $\langle u_i^2 \rangle$] for linear sequences of $N=50\,000$ points. Circles indicate the simulation results. Dots represent analytical results for the variance calculated according to Eq. (A4), which takes into account the finite size effects. The solid line is the variance for $N \rightarrow \infty$. It can be seen that as $\alpha \rightarrow 1$ the convergence becomes slower and finite size effects become more dominant [i.e., the convergence is nonuniform in the range $\alpha \in (0, 1)$].

$$\text{var}(u_i) = \frac{1}{1-\alpha} 2^{2\alpha-2} (1 - N^{2\alpha-2}). \quad (\text{A4})$$

Thus, for $\alpha < 1$ the variance converges, and for $\alpha > 1$ it diverges.

Nonstationarity: For $\alpha \geq 1$ the variance *diverges* with the sequence length N , because of the singularity in the power spectrum, and the sequence is nonstationary. For $\alpha > 1$ the divergence is power-law, i.e., $\text{var}(u_i) \sim N^{2\alpha-2}$, while at $\alpha = 1$ the divergence is logarithmic.

Finite size effects: For $\alpha < 1$ the variance converges to a finite constant so the sequence is stationary, but as $\alpha \rightarrow 1$ this convergence becomes slower. This means that as $\alpha \rightarrow 1$, larger and larger sequence lengths N are required so that the variance will indeed converge to a constant value (see Fig. 7). This argument also holds for other values of the correlation functions $\rho(n)$, $n=0, 1, \dots, \infty$, although in a more moderate way.

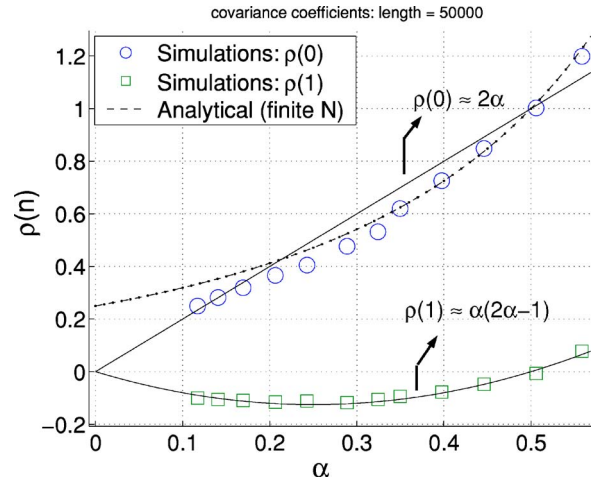


FIG. 8. (Color online) Correlation coefficients $\rho(0) = \langle u_i^2 \rangle$ (circles) and $\rho(1) = \langle u_i u_{i+1} \rangle$ (squares) for linear sequences of 50 000 points, in the range $0 < \alpha < 1/2$. The dashed line indicates the analytical results for $\rho(0)$, taking into account the finite series size effects, which approximately follows results for $N \rightarrow \infty$ (solid line). $\rho(1)$ is negative for $0 < \alpha < 1/2$ indicating anticorrelations. The solid lines are the analytical expressions of Eq. (A5).

The strong finite size effects around $0.75 < \alpha < 1.25$ and the nonstationarity at $\alpha \geq 1$ have to be taken into account when calculating the magnitude series scaling exponent α_v . This is done by dividing the volatility fluctuation function $\text{var}(V_n)$ by the variance of the sequence given in Eq. (A4) [20].

For $N \rightarrow \infty$ the finite size effects disappear and α_v converges to its theoretical value (see Fig. 1). This convergence is extremely slow and becomes weaker as we approach $\alpha \approx 1$.

For completeness, we show in Fig. 8 the correlation coefficients $\rho(n=i-j)$ for $\alpha < 1/2$. In this regime the sequences exhibit short range anticorrelations as can be seen in Fig. 8. The expression of the correlation function for $\alpha < 1/2$ is approximately [8]:

$$\rho(i-j) = \langle u_i u_j \rangle \sim \begin{cases} \alpha(2\alpha-1)|i-j|^{2\alpha-2} & i \neq j \\ 2\alpha & i = j. \end{cases} \quad (\text{A5})$$

[1] M. F. Shlesinger, Ann. N.Y. Acad. Sci. **504**, 214 (1987).
 [2] C.-K. Peng, S. Havlin, H. E. Stanley, and A. L. Goldberger, Chaos **5**, 82 (1995).
 [3] Y. Ashkenazy, P. C. Ivanov, S. Havlin, Chung-K. Peng, A. L. Goldberger, and H. E. Stanley, Phys. Rev. Lett. **86**, 1900 (2001).
 [4] J. Muzy, E. Bacry, and A. Arneodo, Int. J. Bifurcation Chaos Appl. Sci. Eng. **4**, 245 (1994).
 [5] J. Feder, *Fractals* (Plenum, New York, 1988).
 [6] G. Parisi and U. Frisch, in *Turbulence and Predictability in Geophysical Fluid Dynamics, Proc., Int. School E. Fermi*, edited by M. Ghil *et al.*, (North-Holland, Amsterdam, 1985).

[7] J. W. Kantelhardt, S. A. Zschiegner, E. Koscielny-Bunde, S. Havlin, A. Bunde, and H. E. Stanley, Physica A **316**, 87 (2002).
 [8] M. S. Taqqu, V. Teverovsky, and W. Willinger, Fractals **3**, 785 (1995).
 [9] *Fractals in Science*, Springer, 2nd ed., edited by A. Bunde and S. Havlin (Springer, Berlin, 1996).
 [10] C.-K. Peng, S. V. Buldyrev, S. Havlin, M. Simons, H. E. Stanley, and A. L. Goldberger, Phys. Rev. E **49**, 1685 (1994).
 [11] A. Bunde, S. Havlin, J. W. Kantelhardt, T. Penzel, J. H. Peter, and K. Voigt, Phys. Rev. Lett. **85**, 3736 (2000).
 [12] R. Stratonovich, *Topics in the Theory of Random Noise* (Gor-

- don and Breach, New York, 1967), Vol. 1.
- [13] N. G. Van-Kampen, *Stochastic Processes in Physics and Chemistry* (North-Holland, Amsterdam, 1981).
- [14] U. Frisch, *Turbulence* (Cambridge University Press, Cambridge, 1995).
- [15] Y. H. Liu, P. Gopikrishnan, P. Cizeau, M. Meyer, C. K. Peng, and H. E. Stanley, *Phys. Rev. E* **60**, 1390 (1999).
- [16] A. Arneodo, E. Bacry, and J. F. Muzy, *J. Math. Phys.* **39**, 4142 (1998).
- [17] Y. Ashkenazy, S. Havlin, P. C. h. Ivanov, C.-K. Peng, V. Schulte-Frohlinde, and H. E. Stanley, *Physica A* **323**, 19 (2003).
- [18] H. A. Makse, S. Havlin, M. Schwartz, and H. E. Stanley, *Phys. Rev. E* **53**, 5445 (1996).
- [19] It is important to note that in Fig. 1 we use both $|u_i|$ and u_i^2 to calculate the volatility scaling exponent. Nevertheless, the usual method for calculating the volatility scaling exponent is performed by taking the absolute value of the *differences* series, Δu_i , rather than u_i itself [3,17]. The reason for this is that in many cases the given time series has an exponent in the range $\frac{1}{2} < \alpha < 1\frac{1}{2}$. By differentiating the sequence we get a new sequence Δu_i with an exponent $\tilde{\alpha} = \alpha - 1 < \frac{1}{2}$. According to our analysis, if the sequence is linear, the volatility exponent for this series will be $\tilde{\alpha}_v = \frac{1}{2}$ (whereas for the original series α_v may be higher than $\frac{1}{2}$ even for linear data).
- [20] FA and DFA actually measure the scaling of the fluctuations for window sizes ranging from 1 to t . Fluctuations for windows of size t are given by $\langle X_t^2 \rangle$, while fluctuations for windows of size 1 are actually the variance of the sequence. Thus, the scaling exponent is approximated by
- $$\begin{aligned} & [\ln \langle X_t^2 \rangle^{1/2} - \ln \langle X_1^2 \rangle^{1/2}] / \ln t \\ &= [\ln \langle X_t^2 \rangle^{1/2} - \ln \text{var}(u_i)^{1/2}] / \ln t \\ &= \ln[\langle X_t \rangle / \text{var}(u_i)] / 2 \ln t. \end{aligned}$$
- Therefore, in cases where the variance is not constant, the fluctuation function $\langle V_t^2 \rangle$ should be normalized by the variance.
- [21] Note that in the DFA notation the expressions for α should be larger by one than those of [16]; however, since here we consider the increments, the series exponent is reduced back by one, thus compensating the DFA integration.
- [22] T. Schreiber and A. Schmitz, *Physica D* **142**, 346 (2000).
- [23] <http://www.pmel.noaa.gov/tao/realtime.html>.
- [24] E. Bacry, J. Delour, and J. F. Muzy, *Phys. Rev. E* **64**, 026103 (2001).
- [25] S. Lovejoy and D. Schertzer, *Ann. Geophys., Ser. B* **4**, 401 (1986).
- [26] F. Schmitt, S. Lovejoy, and D. Schertzer, *Geophys. Res. Lett.* **22**, 1689 (1995).
- [27] D. C. Lin and R. L. Hughson, *Phys. Rev. Lett.* **86**, 1650 (2000).
- [28] K. Hasselmann, *Tellus* **28**, 473 (1976).